Eur. Phys. J. Appl. Phys. **97**, 18 (2022)
© EDP Sciences, 2022
https://doi.org/10.1051/epjap/2022210282

THE EUROPEAN PHYSICAL JOURNAL APPLIED PHYSICS

Special Issue on 'Nanoalloys: Kinetic and Environmental Behaviour', edited by Pascal Andreazza, Riccardo Ferrando and Liu Xiaoxuan

Regular Article

Central vacancy creation in icosahedral nanoparticles induced by the displacement of large impurities

Diana Nelli*

Dipartimento di Fisica dell'Università di Genova, via Dodecaneso 33, Genova 16146, Italy

Received: 10 December 2021 / Received in final form: 28 January 2022 / Accepted: 1 February 2022

Abstract. We employ metadynamics simulations at room temperature to study the diffusion of large single-atom impurities within otherwise pure icosahedral nanoparticles, for different bimetallic systems (Au-Co, Ag-Co, Ag-Ni, Au-Pt and Au-Rh) and icosahedral sizes. Our simulations reveal that the displacement of the impurity induces the formation of a vacancy in the central part of the structure, as already observed for small icosahedra of Au-Co and Ag-Cu, therefore confirming the generality of this peculiar diffusion process. At the largest size, a new collective displacement mechanism is identified alongside the diffusion of the impurity. For Au-Pt clusters, different diffusion pathways are observed, which are mediated by a partial deformation of the nanoparticle surface. This is due to the lack of stability of fivefold veritices in Pt icosahedral clusters. We prove that the stability of the icosahedral surface is an essential condition for the occurrence of the combined process of impurity diffusion and internal vacancy formation.

1 Introduction

The physical and chemical properties of bimetallic nanoparticles are known to strongly depend on their chemical ordering, i.e. the spatial arrangement of atoms of the two species within the nanoparticle volume. At thermodynamic equilibrium, the nanoparticle chemical ordering reflects the properties of the bimetallic system: systems with a strong tendency to mix in the bulk exhibit mixing chemical ordering patterns also at the nanoscale, whereas in nonmiscible systems different types of phase-separated patterns are observed, such as Janus-like and core-shell [1,2]. However, out-of-equilibrium chemical arrangements are often obtained during nanoparticle growth experiments [3,4]; transformations of the chemical ordering are then observed [5–10], which take place through intra-nanoparticle diffusion of atoms of the two species, and eventually bring to the most favourable configuration.

Atomistic simulations can be of great help to identify the most common atomic diffusion pathways, which are at the basis of chemical ordering transformations observed in the experiments. The problem is indeed not trivial, since diffusion processes at the nanoscale can be quite different from their bulk counterpart. In general, a wider variety of diffusion mechanisms is activated, which involve the partial disordering of the nanoparticle surface [11–13] or are mediated by the presence of internal vacancies [13–16].

Recently, we have described a new diffusion mechanism that may take place in icosahedral nanoparticles, in which the displacement of a single-atom impurity between adjacent internal sites induces the formation of a vacancy in the site originally occupied by the impurity [17]. The spontaneous creation of vacancies in metallic nanoparticles has been observed in previous molecular dynamics works, but, in all cases, vacancies first appear on the nanoparticle surface, and then migrate inwards through subsequent filling steps [13,14,16]. In reference [17] we have shown that vacancies can appear directly in the inner part of the cluster. This peculiar behaviour is due to the presence of non-homogenous compressive stress in the inner part of icosahedral structure, coupled to the lattice mismatch between the atoms of the icosahedral matrix and the impurity.

The combined process of impurity diffusion and vacancy formation has been observed during the migration of a Au atom within perfect Co icosahedra of size 147 and 309, and the case of a Ag atom moving within Cu icosahedra of the same sizes. In both cases the impurity is larger than the atoms of the icosahedral matrix, with a lattice mismatch of 15% and 13%, respectively.

The aim of this article is to investigate whether this type of diffusion mechanism takes place also in other bimetallic systems with similar features, and in icosahedra of bigger sizes. To this end we employ metadynamics simulations, which we have proved to be particularly appropriate for the study of impurity diffusion at room temperature in the case of Au-Co and Ag-Cu systems. Specifically, we study the evolution of Ag-Co, Ag-Ni, Au-Pt and Au-Rh icosahedral nanoparticles of size 147 and 309 and of Au-Co icosahedra of size 561 and 923 from an initial configuration in which the Au/Ag impurity is placed in the central site. Our simulations confirm the generality of the diffusion process identified in reference [17], as well as its relation

* e-mail: nelli@fisica.unige.it

with the pressure profile in the icosahedral structure. In addition, we find that in large icosahedra the collective displacement induced by the diffusion of the impurity takes place somewhat differently than what we observe at smaller sizes. Finally, we identify an important condition required for the occurrence of the combined process of impurity diffusion and internal vacancy formation in bimetallic systems, which is related to the stability of the icosahedral matrix.

2 Model and methods

The atomistic force field for the interaction between atoms in the nanoparticle has been developed by Gupta [18] and by Rosato et al. [19] from the second-moment approximation to the tight-binding model [20]. In the Gupta force field, the binding energy E of the system is written as the sum of single-atom contributions, i.e. $E = \sum_i E_i$, E_i being the energy of the ith atom. Form and details of the force field are given in reference [21]. The parameters of the potential are fitted to the bulk properties of each bimetallic system; specifically, they are taken from: reference [22] for Au-Co, reference [23] for Ag-Cu, reference [24] for Ag-Co and Ag-Ni, references [25] and [26] for Au-Rh.

Metadynamics (MetaD) simulations are performed using our own molecular dynamics (MD) code interfaced with the PLUMED plugin reference [27]. The equations of motion are numerically solved by the velocity Verlet algorithm with a time step of 5 fs, and an Andersen thermostat is employed to keep the temperature constant [28,29]. In addition, the free energy profile of the system is modified during the simulation by a history-dependent repulsive potential. This extra potential is made of Gaussian functions deposited along the simulated trajectory in the space of few properly chosen collective variables (CVs), according to the metadynamics scheme [30]. Here we use the CVs introduced by Pipolo et al. [31], in which the path CVs s and z [32] are combined with the permutation invariant vector (PIV) metric [33]. Further details on the CVs can be found in reference [17], in which we have shown that with a proper choice of the CV parameters it is possible to efficiently accelerate the diffusion of Au and Ag impurities within the icosahedral matrix. The MetaD parameters are as follows: Gaussian height $\delta = 0.10\,\text{eV}$, Gaussian width $(\sigma_s,\sigma_z) = (0.02,0.1)$, and deposition stride $= 10\,\text{ps}$. All MetaD simulations are performed at room temperature (300 K).

The local pressure on a selected atom in the nanoparticle is calculated from its atomic stress tensor, as in reference [34]. All the energy and pressure values reported in the following refer to locally minimized structures.

3 Results and discussion

We consider perfect icosahedral clusters of sizes 147, 309, 561 and 923 atoms. The clusters are completely made of Co, Ni, Pt or Rh, with the exception of a single-atom impurity of Ag (in Co and Ni clusters) or Au (in Co, Pt and Rh clusters). The largest icosahedral sizes (561 and 923) are considered only for Au-Co. In our simulations the impurity is initially placed in the central site of the icosahedron. This starting configuration is energetically unfavourable for all the considered systems; the impurity is therefore expected to diffuse within the cluster volume until reaching the best placement, which turns out to be on the surface in all cases according to our energy calculations, as for the corresponding Au-Co and Ag-Cu clusters of size 147 and 309 [17]. Here we study the very first step of the impurity diffusion, i.e. the displacement from the center to the second icosahedral shell. The driving force for the displacement is the relaxation of compressive stress in the central part of the cluster, as we show in the following.

In Table 1 we show the effect of the impurity displacement on the local pressure in the central site and in the second shell of perfect icosahedra. Data referring to Au-Co and Ag-Cu clusters of size 147 and 309 are taken from reference [17]. In all cases the atomic pressure on the impurity when placed in the central site is considerably large and, as expected, for each bimetallic system it increases with the cluster size [35]. The pressure on the impurity is much lower when it occupies one of the sites in the second shell. The displacement of the impurity also affects its local environment. In general, the pressure on the central site, that is now occupied by a smaller atom, decreases significantly; by contrast, the average pressure on the second shell displays only a minor increase. The decrease of the atomic pressure on the impurity causes an improvement of its single-atom energy in all cases (see the values of ΔE^{imp} in Tab. 1). The overall decrease of compressive stress in the central part of the icosahedron also causes an improvement of the total energy of the cluster (see the values of ΔE in Tab. 1). The only exception is the Au-Rh system, in which the replacement of the Au impurity with a Rh atom in the central site actually causes an increase in the central pressure for both icosahedral sizes, and, as a consequence, also in the total energy.

To study the dynamical process of impurity diffusion from the center to the second shell we employ MetaD simulations at room temperature. Specifically, for sizes 147 and 309 we perform five independent MetaD simulations for each bimetallic system, whereas for Au-Co clusters of sizes 561 and 923 three independent MetaD simulations are performed. The two reference configurations needed to build the path CV are the initial configuration and a configuration in which the impurity is in the third shell. The CV parameters are chosen to ensure a good resolution of intermediate configurations (with the impurity in the second shell) in the CV space; more details on this point can be found in reference [17].

Our simulations show that in Au-Co, Ag-Co, Ag-Ni and Au-Rh systems the displacement of the impurity takes place through the same diffusion mechanism observed for Au-Co and Ag-Cu at size 147 and 309, which we have described in detail in reference [17]. In short, the key points of the process are the following: (i) the impurity moves to the second shell leaving a vacancy in the central site; (ii) the displacement of the impurity induces the collective motion of a row of atoms in the outward direction; (iii) the outer atom of the row is expelled from the

Table 1. Local pressure on the first icosahedral shell, i.e. on the central site (p_1), and on the second shell (p_2) for three different configurations: (i) perfect icosahedron with the impurity in the first shell (initial configuration of our simulations); (ii) perfect icosahedron with the impurity in the second shell; (iii) icosahedron with a central vacancy and an adatom on the surface, with the impurity in the second shell (obtained in our simulations). In cases (ii) and (iii) we report both the average pressure on the second shell ($\bar{p}_2$) and the pressure on the impurity ($p_2^{\rm imp}$). Energy differences between (ii) and (i) and configurations (iii) and (i) are reported, for both the impurity ($\Delta E^{\rm imp}$ and $\Delta E^{\rm imp*}$) and the total cluster (ΔE and ΔE^*). Energies are in eV, pressures in GPa.

Size	system	(i) impurity in 1st shell		(ii) impurity in 2nd shell			$\Delta E^{\rm imp}$	ΔE	(iii) impurity in 2nd shell*			$\Delta E^{\rm imp*}$	ΔE^*
		$p_1^{\rm imp}$	p_2	p_1	$\bar{p}_2$	$p_2^{\rm imp}$			p_1	$\bar{p}_2$	$p_2^{\rm imp}$		
147	Au-Co	48.5	9.6	28.1	10.5	28.2	−0.53	−1.09	-	9.5	25.0	−0.46	−0.57
	Ag-Cu	35.3	9.6	26.0	9.3	21.2	−0.50	−0.66	-	8.8	22.0	−0.44	+0.07
	Ag-Co	54.7	10.1	29.2	11.6	33.0	−0.60	−1.24	-	10.6	28.5	−0.56	−0.74
	Ag-Ni	63.6	11.4	33.9	12.6	30.6	−0.60	−0.84	-	11.5	25.7	−0.51	+0.15
	Au-Pt	69.2	18.0	58.9	19.4	28.5	−0.61	−0.69	-	-	-	-	-
	Au-Rh	54.0	22.7	68.5	23.4	28.5	−0.79	+0.10	-	22.3	26.1	−0.76	+1.54
309	Au-Co	59.3	12.4	29.5	13.2	30.7	−0.53	−1.04	-	12.3	29.4	−0.46	−0.67
	Ag-Cu	43.0	11.8	28.2	11.8	25.1	−0.52	−0.64	-	11.4	26.8	−0.45	−0.08
	Ag-Co	65.2	13.0	31.1	14.4	35.7	−0.61	−1.20	-	13.9	36.3	−0.57	−0.85
	Ag-Ni	72.0	14.6	37.4	15.7	32.8	−0.68	−0.90	-	14.5	28.7	−0.59	−0.17
	Au-Pt	72.0	23.6	61.7	24.9	34.6	−0.61	−0.60	-	-	-	-	-
	Au-Rh	58.9	29.2	80.0	29.8	32.1	−0.85	+0.26	-	28.3	29.5	−0.83	+1.18
561	Au-Co	65.2	13.6	31.1	14.9	34.1	−0.54	−1.08	-	13.5	29.2	−0.47	−0.84
923	Au-Co	69.0	14.7	32.6	16.3	36.5	−0.57	−1.12	-	14.9	31.4	−0.50	−0.99

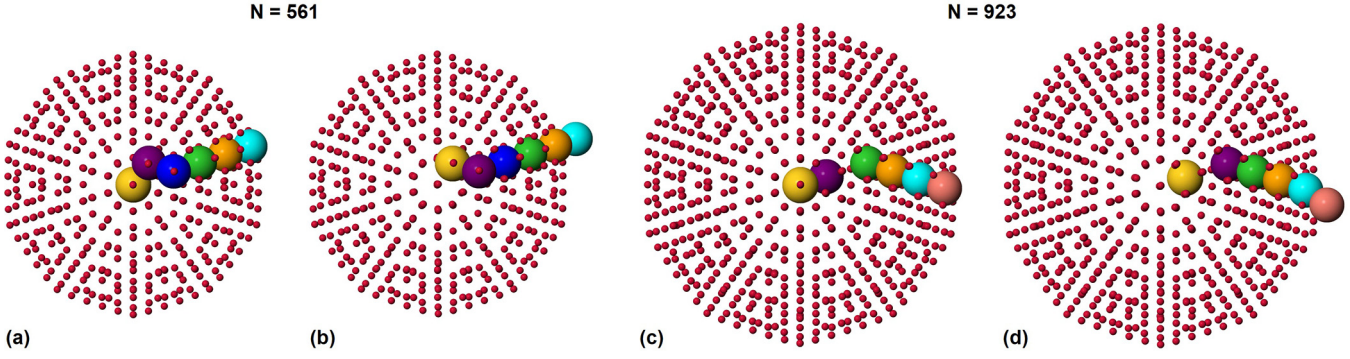

Fig. 1. Snapshots of the migration of the Au impurity from the center to the second shell within Co icosahedral clusters, obtained in MetaD simulations at room temperature. The displacement of the impurity is coupled to the formation of a vacancy in the central site and to the appearance of a Co adatom on the surface. (a and b) Starting and final configuration of the diffusion process for size $N = 561$. (c and d) Same, but for size $N = 923$. Atoms involved in the diffusion process are highlighted.

icosahedron and becomes an adatom; (iv) few atoms are involved in the process and the icosahedral geometry is kept, except for the adatom.

In Figure 1 we show the cluster before and after the impurity diffusion process, for Au-Co icosahedra of size 561 and 923. The Au impurity and the Co atoms involved in the process are displayed as big spheres; the other Co atoms keep their initial positions. At size 561, 6 atoms are involved in the process, one for each icosahedral shell: the Au impurity (displayed in yellow) moves to the second shell, and replaces a Co atom, displayed in purple in Figures 1a and 1b; the atom in purple moves to the third shell, and replaces the atom displayed in blue, which in turn moves to the fourth shell; at the end of the process, one of the surface atoms is pushed off by an atom coming from the subsurface layer, and becomes an adatom (cyan atom in Fig. 1b). The same process is observed in Ag-Co, Ag-Ni and Au-Rh systems; as might be expected, the number of atoms involved in the process depends on the cluster size, and it is equal to the number of icosahedral shells, namely 4 and 5 for size 147 and 309, respectively.

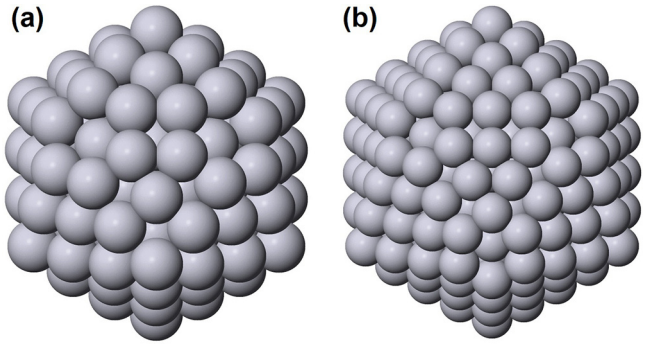

Fig. 2. Most favourable rosette-like reconstructions for Pt icosahedra: (a) icosahedron of size 147, in which two fivefold vertices are replaced by hexagonal rings; (b) icosahedron of size 309, in which three vertices are replaced.

At size 923 we observe the same kind of impurity diffusion and vacancy formation process, but with some difference in the moving atomic row. As we can see in Figures 1c and 1d, the highlighted atomic row is interrupted in correspondence of the third shell: as observed at smaller sizes, the Au impurity replaces one of the atoms in the second shell, but this atom (in purple) passes through the third shell and stops in the fourth shell, where it replaces the green atom. The third shell is unchanged at the end of the process. This behaviour is observed in all our simulations, with different positions of the interruption in the atomic row.

In Table 1 we report pressure and energy values for the outcomes of the diffusion processes. Values of atomic pressure on the impurity and of average pressure in the second shell are generally lower than those obtained when the impurity is placed in the second shell of the perfect icosahedron, without the central vacancy. In addition, the removal of the highly compressed central atom largely reduces the overall inner pressure of the structure [36]. As already discussed, stress relaxation is energetically advantageous; however, the creation of an internal vacancy and of an adatom on the surface reduces the number of atomic bonds, which has the opposite effect on the total energy of the cluster. The energy balance depends on the system and on the cluster size: in some cases the diffusion of the impurity lowers the total energy of the cluster, in other cases the energy increases. However, we notice that the atomic energy of the impurity considerably improves in all cases after the diffusion (see $\Delta E^{\mathrm{imp}*}$ in Tab. 1).

Data in Table 1 suggest that the combined process of impurity diffusion and vacancy formation cannot be explained by means of energetic considerations on the whole nanoparticle, but it is instead due to a local release of compressive stress in the innermost sites, in the proximity of the impurity.

The diffusion pathway described above is not observed in the case of Au-Pt clusters. In all our MetaD simulations the Pt icosahedral matrix partially deforms while the Au impurity is still in the central site. The impurity then diffuses outwards within such deformed region; when the first step of the diffusion is completed, the cluster sometimes restores the perfect icosahedral geometry, with the impurity in the second shell; in other cases, surface defects are not completely eliminated. In some simulations we observe vacancy-mediated diffusion pathways, with the vacancy first appearing in the subsurface layer on the disordered side of the cluster; the vacancy then migrates inward until it reaches the second shell, and it is filled by the Au atom coming from the central site. If the impurity is not replaced by any of the surrounding atoms, a vacancy appears in the center. However, the vacancy creation process is rather different from what observed in the other bimetallic systems: in this case the vacancy first appears on the surface and then is displaced to the central site during a multi-step process, in which many atoms are involved.

Deformation-mediated diffusion processes have been observed also in Au-Co and Ag-Cu icosahedral clusters of size 147, in MD simulations at 600-700 K [16,17]. In the case of Au-Pt, the activation of such processes at room temperature is due to the instability of the perfect icosahedral geometry. The tendency to surface deformation has indeed been observed for pure Pt icosahedral clusters; specifically, some surface reconstruction patterns have been proved to be energetically favourable. In the reconstructed surface, one or more fivefold vertices are transformed into a so-called rosette, i.e. a hexagonal ring [37]. The most favourable rosette-like reconstructions for Pt icosahedra of size 147 and 309 are shown in Figure 2.

To check the stability of the icosahedral matrix, the energy of the structures of Figure 2 is evaluated for pure Co, Cu, Ni, Pt and Rh, and it is compared to the energy of the perfect icosahedra of the same size. Data are reported in Table 2. In all cases the reconstruction of the icosahedral surface is largely energetically unfavourable, expect for Pt clusters, in which the presence of rosette motifs lowers the total energy of the cluster. Energy calculations are in agreement with the results of MetaD simulations, in which the disordering of the surface at room temperature is observed only for Au-Pt. Our results show that the stability of the icosahedral matrix against surface reconstruction is essential for the observation of the combined process of impurity diffusion and central vacancy formation. If the icosahedral surface is unstable, other pathways are more likely, in which the structure is partially deformed. We point out that our simulations are able to reproduce both types of diffusion processes; this further confirms the efficiency of the employed MetaD scheme in the study of the diffusion of impurities within nanoparticles.

4 Conclusions

In this article we have studied the diffusion of a single-atom impurity within otherwise pure icosahedral clusters. We have considered different bimetallic systems, in which the impurity is larger than the atoms of the icosahedral matrix, and different icosahedral sizes. In our simulations we have observed the same diffusion mechanism first described in reference [17], in which the displacement of the impurity is coupled to the creation of an internal

Table 2. Energy difference between icosahedra displaying the rosette-like surface reconstructions shown in Figure 2 and perfect icosahedra of the same size. Data refer to pure clusters. Energies are in eV.

Size			147					309		
System	Co	Cu	Ni	Pt	Rh	Co	Cu	Ni	Pt	Rh
$E_{\text{rosette}} - E_{\text{ico}}$	+0.58	+1.41	+2.09	−0.22	+4.05	+0.73	+1.96	+2.93	−0.54	+5.54

vacancy. This mechanism was previously observed in the evolution of Au-Co and Ag-Cu clusters of size 147 and 309, while its possible occurrence in other similar systems was only suggested. Our results show that it may indeed take place in other bimetallic systems and in cluster of larger sizes, being therefore a general mechanism for the diffusion of large impurities within icosahedral nanoparticles.

The driving force behind the observed diffusion process is the relaxation of compressive stress in the central part of the icosahedral structure, which is achieved in all cases, whereas the effect on the total energy of the cluster depends on the system and on the nanoparticle size.

At the largest icosahedral size, a new collective displacement mechanism is identified alongside the diffusion of the impurity. The outcome of the process is the same as at smaller sizes, but one of the atoms involved in the process undergoes a larger displacement, as it does not replace any of its neighbouring atoms in the outer shell, but passes through it. By contrast, the atoms of that shell keep their initial positions.

Our simulation and energy evaluations show that, in addition to the lattice mismatch between the impurity and the atoms belonging to the icosahedral matrix, the stability of the surface is needed for the appearance of the vacancy directly in the central site, alongside the displacement of the impurity. If the reconstruction of the surface is energetically favourable, deformations of the icosahedral matrix are observed also at room temperature, and different diffusion pathways take place.

The author acknowledges support from the PRIN 2017 project UTFROM of the Italian MIUR and from the Progetto di Eccellenza of the Physics Department of the University of Genoa, and networking support from the IRN Nanoalloys of CNRS. The author would like to thank Riccardo Ferrando for useful discussion and Fabio Pietrucci for assistance with metadynamics simulations.

References

1. R. Ferrando, J. Jellinek, R.L. Johnston, Chem. Rev. **108**, 845 (2008)
2. R. Ferrando, *Structure and Properties of Nanoalloys*, Frontiers of Nanoscience, Volume 10 (Elsevier, 2016)
3. T.W. Liao, A. Yadav, K.J. Hu, J. van der Tol, S. Cosentino, F. D'Acapito, R.E. Palmer, C. Lenardi, R. Ferrando, D. Grandjean et al., Nanoscale **10**, 6684 (2018)
4. D. Nelli, A. Krishnadas, R. Ferrando, C. Minnai, J. Phys. Chem. C **124**, 14338 (2020)
5. S. Liu, Z. Sun, Q. Liu, L. Wu, Y. Huang, T. Yao, J. Zhang, T. Hu, M. Ge, F. Hu et al., ACS Nano **8**, 1886 (2014)
6. M. Chi, C. Wang, Y. Lei, G. Wang, D. Li, K.L. More, A. Lupini, L.F. Allard, N.M. Markovic, V.R. Stamenkovic, Nat. Commun. **6**, 8925 (2015)
7. C.S. Bonifacio, S. Carenco, C.H. Wu, S.D. House, H. Bluhm, J.C. Yang, Chem. Mater. **27**, 6960 (2015)
8. M. Tang, B. Zhu, J. Meng, X. Zhang, W. Yuan, Z. Zhang, Y. Gao, Y. Wang, Mater. Today Nano **1**, 41 (2018)
9. M. Schnedlitz, D. Knez, M. Lasserus, F. Hofer, R. Fernández-Perea, A.W. Hauser, M. Pilar de Lara-Castells, W.E. Ernst, J. Phys. Chem. C **124**, 16680 (2020)
10. F. Li, Y. Zong, Y. Ma, M. Wang, W. Shang, P. Tao, C. Song, T. Deng, H. Zhu, J. Wu, ACS Nano **15**, 5284 (2021)
11. Y. Shimizu, S. Sawada, K.S. Ikeda, Eur. Phys. J. D **4**, 365 (1998)
12. Y. Shimizu, K.S. Ikeda, S.i. Sawada, Phys. Rev. B **64**, 075412 (2001)
13. T. Niiyama, S. Sawada, K.S. Ikeda, Y. Shimizu, Chem. Phys. Lett. **503**, 252 (2011)
14. F. Delogu, Nanotechnology **18**, 235706 (2007)
15. T. Shibata, B.A. Bunker, Z. Zhang, D. Meisel, C.F. Vardeman, J.D. Gezelter, J. Am. Chem. Soc. **124**, 11989 (2002)
16. R. Ferrando, Diffus. found. **12**, 23 (2017)
17. D. Nelli, F. Pietrucci, R. Ferrando, J. Chem. Phys. **155**, 144304 (2021)
18. R.P. Gupta, Phys. Rev. B **23**, 6265 (1981)
19. V. Rosato, M. Guillopé, B. Legrand, Philos. Mag. A **59**, 321 (1989)
20. F. Cyrot-Lackmann, F. Ducastelle, Phys. Rev. B **4**, 2406 (1971)
21. D. Nelli, R. Ferrando, Nanoscale **11**, 13040 (2019)
22. A. Rapallo, J.A. Olmos-Asar, O.A. Oviedo, M. Luduena, R. Ferrando, M.M. Mariscal, J. Phys. Chem. C **116**, 17210 (2012)
23. F. Baletto, C. Mottet, R. Ferrando, Phys. Rev. B **66**, 155420 (2002)
24. Z. Kuntová, G. Rossi, R. Ferrando, Phys. Rev. B **77**, 205431 (2008)
25. D. Bochicchio, F. Negro, R. Ferrando, Comput. Theor. Chem. **1021**, 177 (2013)
26. G. Rossi, R. Ferrando, Comput. Theor. Chem. **1107**, 66 (2017)
27. G.A. Tribello, M. Bonomi, D. Branduardi, C. Camilloni, G. Bussi, Comput. Phys. Commun. **185**, 604 (2014)
28. M.P. Allen, D.J. Tildesley, *Computer Simulation of Liquids* (Clarendon, Oxford, 1987)
29. F. Baletto, C. Mottet, R. Ferrando, Surf. Sci. **446**, 31 (2000)
30. G. Bussi, A. Laio, Nat. Rev. Phys. **2**, 200 (2020)
31. S. Pipolo, M. Salanne, G. Ferlat, S. Klotz, A.M. Saitta, F. Pietrucci, Phys. Rev. Lett. **119**, 245701 (2017)
32. D. Branduardi, F.L. Gervasio, M. Parrinello, J. Chem. Phys. **126**, 054103 (2007)

33. G.A. Gallet, F. Pietrucci, J. Chem. Phys. **139**, 074101 (2013)
34. R. Ferrando, J. Phys.: Condens. Matter **27**, 013003 (2015)
35. C. Mottet, G. Rossi, F. Baletto, R. Ferrando, Phys. Rev. Lett. **95**, 035501 (2005)
36. C. Mottet, G. Tréglia, B. Legrand, Surf. Sci. **383**, L719 (1997)
37. E. Aprà, F. Baletto, R. Ferrando, A. Fortunelli, Phys. Rev. Lett. **93**, 065502 (2004)

Cite this article as: Diana Nelli, Central vacancy creation in icosahedral nanoparticles induced by the displacement of large impurities, Eur. Phys. J. Appl. Phys. **97**, 18 (2022)